

International Conference on Space Optics—ICSO 2008

Toulouse, France

14–17 October 2008

Edited by Josiane Costeraste, Errico Armandillo, and Nikos Karafolas



Highly-efficient, frequency-tripled Nd:YAG laser for spaceborne LIDARs

R. Treichel

H.-D. Hoffmann

J. Luttmann

V. Morasch

et al.



HIGHLY-EFFICIENT, FREQUENCY-TRIPLED ND:YAG LASER FOR SPACEBORNE LIDARS

R. Treichel⁽¹⁾, H.-D. Hoffmann⁽²⁾, J. Luttmann⁽²⁾, V. Morasch⁽²⁾, K. Nicklaus⁽²⁾, C. Wührer⁽³⁾

⁽¹⁾EADS Astrium GmbH, 88039 Friedrichshafen, Germany, E-mail:rainer.treichel@astrium.eads.net

⁽²⁾Fraunhofer Institute for Laser Technology, Steinbachstraße 15, 52074 Aachen, Germany, E-mail:hansdieter.hoffmann@ilt.fraunhofer.de

⁽³⁾EADS Astrium GmbH, 81633 München, Germany, E-mail:christian.wuehrer@astrium.eads.net

ABSTRACT

For a spaceborne lidar a highly reliable, long living and efficient laser source is absolutely essential. Within the frame of the development of a laser source for the backscatter lidar ATLID, which will be flown on EarthCare mission, we setup and tested a pre-development model of an injection-seeded, diode pumped, frequency tripled, pulsed high power Nd:YAG MOPA laser operating nominally at 100 Hz pulse repetition frequency. We also tested the burst operation mode. The excellent measured performance parameter will be introduced.

The oscillator rod is longitudinally pumped from both sides. The oscillator has been operated with three cavity control methods: "Cavity Dither", "Pound-Drever-Hall" and "Adaptive Ramp & Fire". Especially the latter method is very suitable to operate the laser in harsh vibrating environment such in airplanes.

The amplifier bases on the InnoSlab design concept. The constant keeping of a moderate fluence in the InnoSlab crystal permits excellent possibilities to scale the pulse energy to several 100 mJ. An innovative pump unit and optics makes the laser performance insensitive to inhomogeneous diode degradation and allows switching of additional redundant diodes.

Further key features have been implemented in a FM design concept. The operational lifetime is extended by the implementation of internal redundancies for the most critical parts. The reliability is increased due to the higher margin onto the laser induced damage threshold by a pressurized housing. Additionally air-to-vacuum effects becomes obsolete. A high efficient heat removal concept has been implemented.

1. INTRODUCTION

One of the most critical subsystems for a spaceborne lidar is the laser transmitter, which has to provide highly stable single frequency laser pulses of high energy. Unfortunately conventional laser designs are doing this at comparable low efficiency. That means

that most of the input energy is wasted there, where high precision optics shall produce a stable spatial and spectral laser pulse. In addition this wasted energy requires a large amount of resources, respectively.

In 2005 ESA initiated a study to pre-develop an efficient laser with performance requirements adapted for the backscatter lidar, ATLID, which will be flown on EarthCare. Goal of this study was to demonstrate the laser performance on a pre-development model (PDM) and to develop a flight model (FM) design concept. Key requirements were among others the optical-optical efficiency and an operational lifetime of 3 years in orbit, which corresponds to an operation with 10 Giga-shots.

Table 1 summarizes the most important performance requirements - all specified for the UV output pulse.

Table 1: Main ATLAS requirements @ 355 nm

Parameters	Requirements
Output energy	23 mJ
Optical-optical efficiency	6 % (8 % target)
Energy short term stability	< ±10 % over 1.4 sec
Polarization	Linear 100:1
Spatial beam quality	$M^2 < 4$
Boresight stability	< ±1/6 of full beam divergence over 1.4 sec
Pulse duration (FWHM)	< 35ns
Longitudinal mode	Single
Pulse linewidth (FWHM)	< 50MHz
Frequency stability	<10 MHz rms over 1.4 sec

2. FUNDAMENTAL DESIGN GOALS

A high power laser for spaceborne lidars should aspire to three fundamental design goals:

- High Efficiency
- Long Lifetime
- High Reliability

Especially the advantages of the high efficiency are manifold. It leads directly to less electrical power consumption and therefore to less solar panel size & mass, less cooling power, less electronics mass, less thermal stress inside of the laser crystals, less thermal gradients in the laser structure, less radiator size & mass, less thermal lenses and better laser performance parameter such beam quality, pointing and energy stability.

As consequence a higher efficiency will also positively take influence on the two other goals, lifetime and reliability, too.

Currently the best heritage has the diode pumped solid state laser in a master oscillator power amplifier(s) configuration (MOPA).

That means that for optimum efficiency and high performance the laser design has to be focused on the amplifier design, because it is the element in the laser system, which consumes and dissipates most of the power.

3. PRE-DEVELOPMENT MODEL SETUP

The overall laser concept is shown in Fig. 1. The laser system is sub-divided into a reference laser, a power laser head and the power laser electronics. The reference laser generates a stable but tunable single laser frequency, which is seeded into the oscillator in the power laser head. The oscillator delivers pulses at 1064 nm with all required temporal, spatial and spectral beam qualities. The subsequent amplifier raises the energy of the laser pulses without significantly changing the beam quality. By converting part of the infrared beam to 532 nm (SHG) and mixing both to 355 nm (THG) the UV beam is generated (Higher Harmonic Generation - HHG). The laser electronics consists of commercial units. The cooling was performed via customized interfaces by a water chiller.

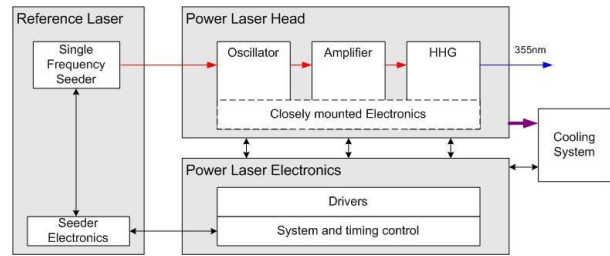


Fig. 1: Functional block diagram of the ATLID laser source

3.1 Oscillator Setup

Fig. 2 shows a picture of the laboratory setup. As reference laser a Mephisto from Innolight was used. A Faraday isolator, which also serves as extraction point for the cavity control signal, avoids interferences from the oscillator into the seed laser. The seed beam is mode matched and coupled into the cavity via the end mirror. The cavity length adaptation for frequency stabilization is done by a piezo actuator mounted to the end mirror. The cavity was controlled with following three methods: Cavity Dither (CD), Pound-Drever-Hall (PDH) and Adaptive Ramp & Fire (ARF). The latter method allows synchronized laser shots.

The 750 mm long oscillator cavity is set up in a folded, end pumped configuration. The pump pulses of 190 μ s duration are delivered via MM-fiber from two modules with two diodes each to the end faces of the Nd:YAG rod, which is mounted in a passively cooled copper heat sink. Q-switching is done with a polarizer and a BBO Pockels cell. To prevent spatial hole burning and achieve a stable single frequency operation two quarterwave plates ensure a twisted mode inside the laser crystal. The 70 % outcoupler mirror is mounted onto a second piezo actuator to induce well-defined cavity length disturbances for vibration sensitivity tests on the cavity control methods.

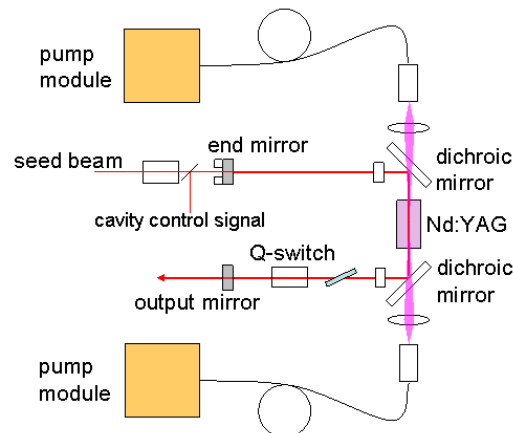


Fig. 2: Scheme of the oscillator

3.2 Amplifier

The amplifier bases on the InnoSlab concept, developed at ILT, which is ideal for high energy and high efficiency amplifiers. It consists of two pump units, here called optical stacks, two pump beam optics, the laser crystal and the signal beam optics.

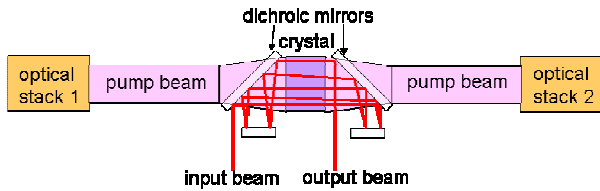


Fig. 3: Functional diagram of the amplifier

The slab crystal is end pumped from two sides (see Fig. 3 and Fig. 7). The advantage is that only two small sized surfaces of the crystal need to be optically polished. The Nd:YAG slab crystal is soldered onto two copper heat sinks (see Fig. 4), which are assembled and mounted onto a thermal interface. The heat sinks are designed to ensure a homogenous temperature distribution along the slab width (x-direction) and a symmetric distribution, resulting in a symmetric thermal lens in the y-direction.

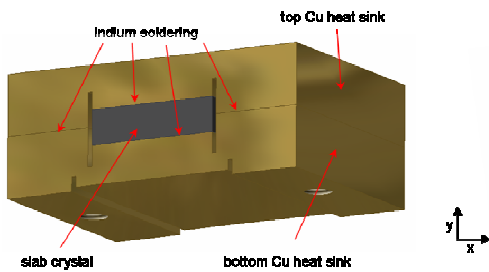


Fig. 4: Soldered slab (15x4x25 mm³) in copper heat sink

I.e. four of the six crystal surfaces are optically unused and are therefore roughened to optimally prevent internal parasitic laser oscillations.

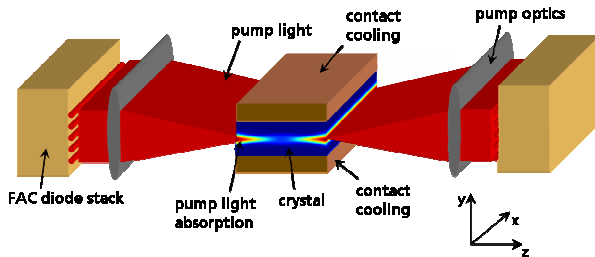


Fig. 5: The InnoSlab concept

To operate the InnoSlab laser as amplifier the signal beam is multiple folded in a single pass configuration

through the crystal (see Fig. 7). By choosing appropriate mirror radii and signal beam divergence the beam is widened in one axis with every pass, the fluence is kept constant and remains always far away from the damage threshold. Fig. 6 shows the signal beam profile before the 1st and after the 3rd, 5th and 7th pass through the slab crystal. As intended the beam diameter stays constant in y-direction and gets wider in x-direction.

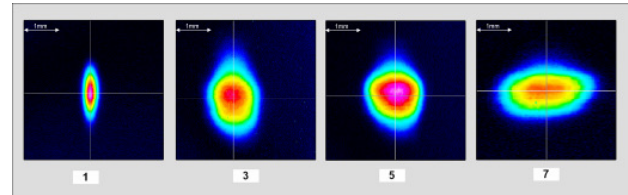


Fig. 6: Beam profile before first and after the third, fifth and seventh path

In principle by adapting the slab crystal width and the number of passes the InnoSlab amplifier is scalable in its output power.

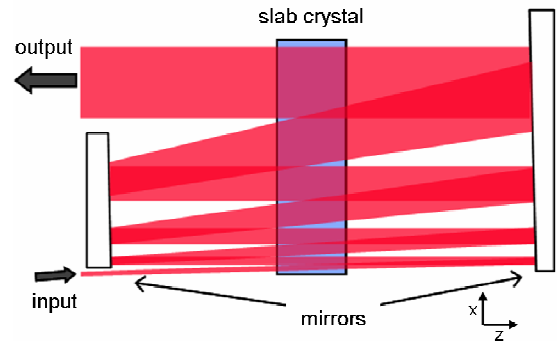


Fig. 7: Beam path of a positive confocal InnoSlab folded single pass amplifier

The amplifier crystal will be pumped by an array of fast axis collimated bars, which are optically combined by stepped mirrors (Fig. 8). The bars have a nominal current of 120 A each, but were operated between 70 A and 80 A. The cooling of each bar is very efficient. This pumping scheme also allows to implement switchable redundancy by additional bars or additional optical stacks.

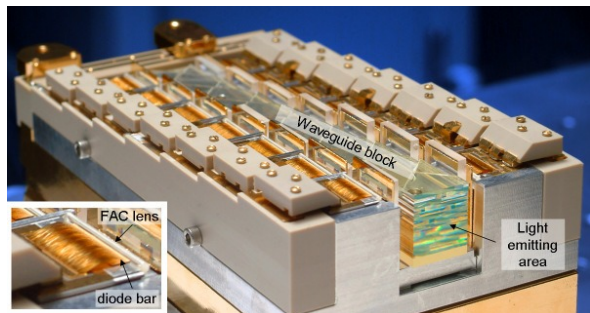


Fig. 8: Optical stack with 14 FAC bars from JOLD, optically stacked with a waveguide block

The pump beam after the waveguide plates is imaged by cylindrical lenses in slow-axis into a homogenizer, which mixes the light of the diodes by total internal reflection. Afterwards the homogenous distribution in slow-axis direction is imaged into the input face of the slab, while in fast-axis direction the light is focused into the center of the slab. The great advantage is that the homogeneous pump light distribution is now insensitive against diode degradation (emitter failure).

3.3 High Harmonic Generation (HHG)

After amplification in the slab the elliptical beam is formed by 2 pairs of cylindrical lenses to get it circular again with an optimum diameter for the frequency conversion. For the second and third harmonic generation LBO crystals were used, each is held in a mount with controlled heating elements that keep the crystals' temperature at 40.0°C. The crystals are cut for critical phase-matching in type I configuration for SHG and type II for THG.

4. PRE-DEVELOPMENT MODEL TEST RESULTS

4.1 Oscillator Test Results

Table 2 summarizes the experimental characterization of the oscillator setup.

The frequency stability of three different cavity control methods has been tested. With the help of the already mentioned second piezo at the output coupler certain disturbances were applied and the achieved frequency stability has been measured.

Table 2: Oscillator test results (IR)

Parameter	Measurement		
Energy of output pulses E_{osc}	7.9 mJ		
Optical-optical efficiency $\eta_{o,osc}$	15.5 % (including pump fiber transfer efficiency of 70 %)		
Energy short term stability	< ± 1.6 % (peak-to-peak over 1.4 s)		
Spatial beam quality	$M^2 < 1.15$		
Pulse duration (FWHM)	36 ns		
Pulse linewidth (FWHM)	< 15 MHz		
Frequency Stability in MHz (rms) in the IR	CD	PDH	ARF
No disturbance	0.93	0.84	< 0.5
f=400 Hz, A=20 nm	1.73	1.62	-
f=1 Hz, A=500 nm	2.84	1.41	-
f=1050 Hz, A=160 nm	-	-	< 1.5

4.2 Amplifier Test Results

The tests on the amplifier performance were carried out with 190 μ s pump pulse duration. The slab crystal had a Nd doping level of 0.8 %. With the slab amplifier pulse energies up to 85 mJ are reached, for higher pump currents the bending of the curves in Fig. 9 indicates the onset of parasitic laser effects in the amplifier cavity. The optical-optical efficiency of 21 % is close to the expected value. Fig. 10 shows the gain curves of the amplifier.

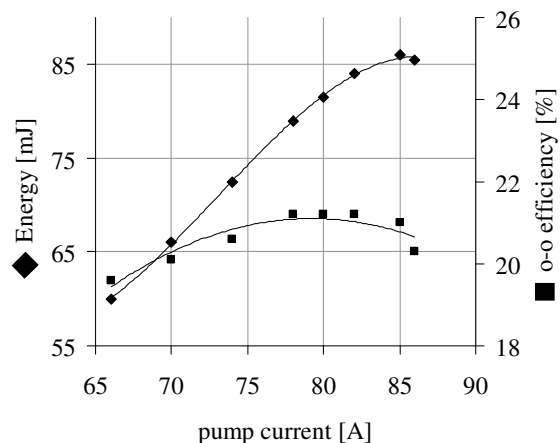


Fig. 9. Amplifier output energy (♦) and optical-optical efficiency (■) vs. pump current

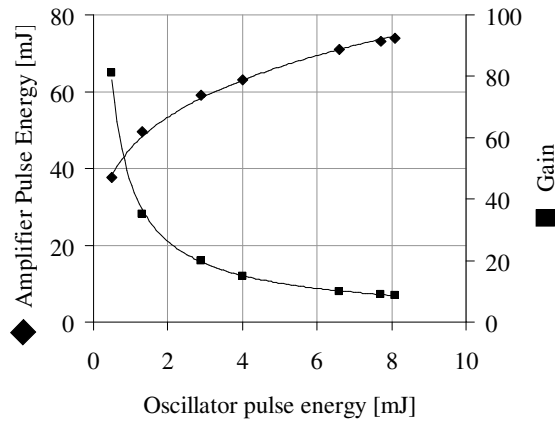


Fig. 10. Amplifier output energy (◆) and gain (■) vs. oscillator pulse energy at 74 A pump current

Due to a slightly asymmetric gain region in y-direction the profile gets a little distorted. This decreases the beam quality slightly. The transversal beam profile is shown in Fig. 11.

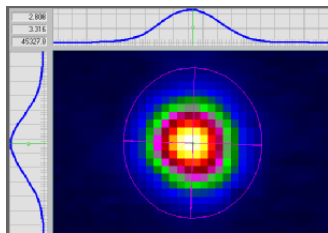


Fig. 11: Beam profile after amplifier

Table 3 summarizes the test results for the amplifier.

Table 3: Amplifier test results

Parameter	Measurement
Output energy per pulse E_{amp}	< 85 mJ
o-o efficiency $\eta_{o-o,amp}$	21 %
Energy short term stability	< ± 2 % (peak-to-peak over 1.4 s)
Spatial beam quality	$M^2_x < 1.55, M^2_y < 1.35$
Pulse duration (FWHM)	30 ns
Pulse linewidth (FWHM)	< 17 MHz

4.3 UV Test Results

Thanks to the good beam quality after the amplifier a very efficient frequency conversion into the UV is possible. Measurements with different amplifier pump

currents, signal beam diameters and SHG crystal lengths were conducted. In Table 4 the results show that it is possible to adapt the laser output to the specific needs such as maximum output energy, longest pulses or safest margin to laser damage.

Table 4: UV laser output test results

		Parameter set for		
		best efficiency	longest pulses	lowest fluence
Output energy per pulse	mJ	33.5	24.3	28.7
Efficiency η_{HHG}	%	50.7	37.2	36.3
Optical-optical efficiency η_{o-o}	%	11.5	8.5	8.2
Short-term energy stability (p-p over 1.4 s)	%	± 2.4	± 1.5	± 4.7
Pulse duration (FWHM)	ns	24.9	33.2	31.7
Fluence of UV pulse on THG crystal	MW/cm ²	<370	<220	<80

In all three cases the beam quality decreased a bit to $M^2_x < 1.7$ and $M^2_y < 1.6$. A picture of the UV beam profile in the focus of a caustic is shown in Fig. 12.

A measurement of the boresight stability over 10 min showed pointing fluctuations of less than ± 14 % of the full beam divergence.

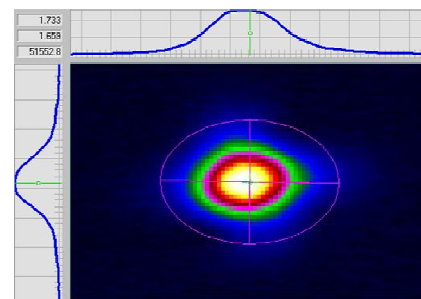


Fig. 12: Focus beam profile of the UV signal

4.4 Results in Burst Mode

Although the development focused on the ATLID transmitter requirements, we tested the operation of the PDM in the ALADIN/AEOLUS burst scenario without any hardware modifications, except the trigger pulse generator for burst mode operation.

The burst mode for ALADIN is specified to:

- cycle period 28 sec
- full performance data acquisition time 7 sec

- less as possible time pre-lasing in order to achieve full performance
- rest of cycle period no lasing

Fig. 13 and Fig. 14 show the output energy after the amplifier and the HHG correspondingly. It can be seen that after 1 sec the IR signal and after 1.5 sec the UV signal is within the specification. This is significantly faster compared to existing laser designs (5s pre-lasing at ALADIN/AEOLUS).

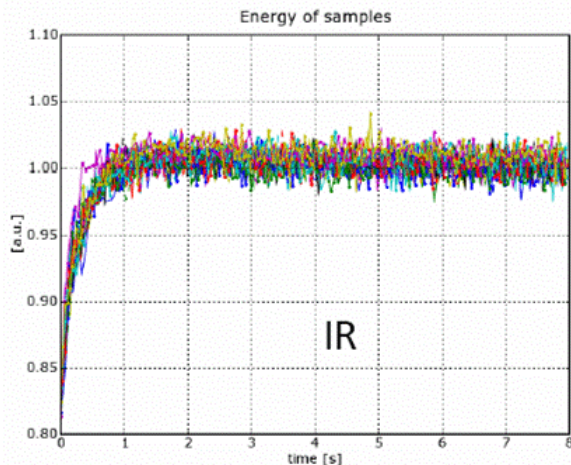


Fig. 13. Output energy after the amplifier within an 8 sec burst

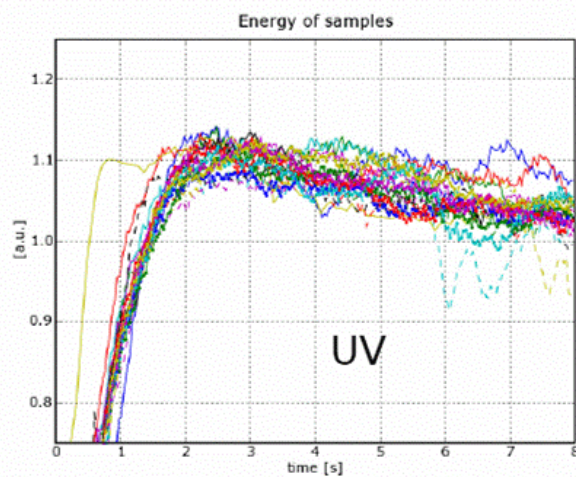


Fig. 14. Output energy in the UV within an 8 sec burst

5. THE FM DESIGN CONCEPT

In order to meet the fundamental design goals we pursued the following design rules for the FM concept of the power laser head:

- Use of the patented InnoSlab concept, developed by ILT, in order to benefit from the excellent efficiency and beam quality
- Implementation of internal redundancy for the most critical parts in order to extend the lifetime
- Operation of the laser in a pressurized housing*, in order to profit from the more reliable environment

Further, in order to optimize the heat removal efficiency loop heat pipes (LHPs) transport the heat directly to the radiator. This is possible, because the tubes are routed through the wall of the pressurized housing. The necessary tightness not only for the LHPs but also all other feedthroughs can be achieved by a dedicated soldering and welding technology.

Redundancy is foreseen for all lifetime critical parts such as pump units of oscillator and amplifier as well as for the tripler and the piezo.

Due to the fact that the optical stack together with its pump optics delivers always a homogeneous pump profile in case of failure of single emitters or bars - only the pump energy drops down. Therefore individual "banks", which are serial circuited bars can be switched on and off.

Similar is the redundancy given in the oscillator pump module. Individual bars can be switch on and off. They are coupled by polarization and geometrically via nearly loss-free fiber coupler.

The tripler output coating is the most critical coating in the laser. It has to have maximum possible transmission at all three wavelengths: 1064 nm, 532 nm and 355 nm. In addition the fluence is relative high and the UV radiation leads to the well known ageing of this optical element. Because the phase matching of the tripler crystal is sensitive only to one axis the exchange from one to the other crystal is performed by a high precision rotational micro-mechanism equipped with three crystals. The mechanism is characterized by high self locking capability, high precision adjustability and very small dimensions. With the temperature variation of the tripler crystal a redundant phase matching fine tuning capability is given.

The piezo is also a critical part. Therefore both resonator mirrors will be equipped with piezos. One works as nominal the other as redundant part.

* Note: At that stage the pressurized housing was not an ESA requirement

The encapsulation of the laser into a pressurized housing filled with dry air at ambient pressure has advantages and avoids several disadvantages for operation in vacuum:

- The air serves as buffer medium for the UV-generated ions.
- The oxygen helps to anneal defects in the coating.
- Any optical air-to-vacuum effects become obsolete.
- Thermal conductance of contact surfaces does not change.
- The air pressure suppresses out gassing.
- The laser induced damage threshold of coatings does not drop by about 10 % to 20 % compared to vacuum.
- The current best knowledge bases on dry air. However, other gas compositions may be equal or even better, but it is an extensive process to research and to find them.

The advantages have to be paid by some disadvantages:

- Electrical power and signals, heat, laser light has to be fed through the pressurized housing walls.
- A careful opto-mechanical design has to be established in order to avoid distortion on the laser optics as soon as the laser will be released in the vacuum.
- The mass and the volume increase.
- Due to the gravity and consequently the appearance of convection a perfect truthful thermal test on ground is not possible.

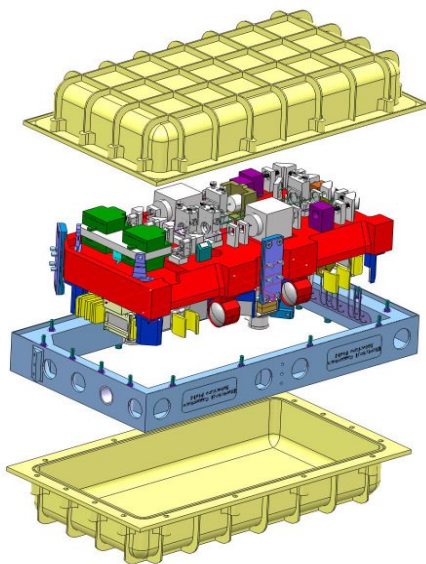


Fig. 15: Design for a flight model of the laser system (exploded view) - red: the laser baseplate with optics on both sides, blue: the frame, yellow: the top and bottom covers

For the design of the power laser head the following physical properties and budgets have been determined:

- Overall dimension: 452 x 252 x 180 mm³
- Mass: 19.2 kg
- Power consumption: 79.9 W

6. CONCLUSION AND OUTLOOK

Within this ATLAS PDM study a laser with superb performance parameters has been developed and demonstrated. It easily meets all optical performance requirements and its efficiency exceeds the performance - to our knowledge - of any other competitor in the world.

Further an ATLAS FM design concept has been developed, which needs a minimum of resources such as power, volume, mass and radiator size. It contains an internal redundancy concept of critical parts (pump diodes, tripler crystal, piezo), which helps to keep the laser operation nominal in case of failure and to extend the overall laser lifetime significantly.

Meanwhile the pump diode development experienced further progress. The size of the pump diodes could be drastically miniaturized at even more output power. Another very attractive and even smaller pump module is now available: The vertical stack inclusive fast axis collimation. The future laser design and the laser lifetime will benefit from this progress.

7. ACKNOWLEDGEMENTS

This work was financed within the European Space Agency's (ESA) frame contract concerning "Breadboarding of Critical Technologies for Future LIDAR Instruments".

The specific work for investigation of the different cavity control methods and the burst mode investigations were financed by DLR.